

Unique Cell Surface Expression of Receptor Tyrosine Kinase ROR1 in Human B-Cell Chronic Lymphocytic Leukemia

Sivasubramanian Baskar,¹ Ka Yin Kwong,¹ Thomas Hofer,¹ Jessica M. Levy,¹ Michael G. Kennedy,¹ Elinor Lee,³ Louis M. Staudt,² Wyndham H. Wilson,² Adrian Wiestner,³ and Christoph Rader¹

Abstract Purpose: Gene expression profiling identified receptor tyrosine kinase ROR1, an embryonic protein involved in organogenesis, as a signature gene in B-cell chronic lymphocytic leukemia (B-CLL). To assess the suitability of ROR1 as a cell surface antigen for targeted therapy of B-CLL, we carried out a comprehensive analysis of ROR1 protein expression. **Experimental Design:** Peripheral blood mononuclear cells, sera, and other adult tissues from B-CLL patients and healthy donors were analyzed qualitatively and quantitatively for ROR1 protein expression by flow cytometry, cell surface biotinylation, Western blotting, and ELISA. **Results:** ROR1 protein is selectively expressed on the surface of B-CLL cells, whereas normal B cells, other normal blood cells, and normal adult tissues do not express cell surface ROR1. Moreover, cell surface expression of ROR1 is uniform and constitutive, i.e., independent of anatomic niches, independent of biological and clinical heterogeneity of B-CLL, independent of B-cell activation, and found at similar levels in all B-CLL samples tested. The antibody binding capacity of B-CLL cell surface ROR1 was determined to be in the range of 10^3 to 10^4 molecules per cell. A portion of B-CLL cell surface ROR1 was actively internalized upon antibody binding. Soluble ROR1 protein was detectable in sera of <25% of B-CLL patients and a similar fraction of healthy donors at concentrations below 200 ng/mL. **Conclusions:** The restricted, uniform, and constitutive cell surface expression of ROR1 protein in B-CLL provides a strong incentive for the development of targeted therapeutics such as monoclonal antibodies.

B-cell chronic lymphocytic leukemia (B-CLL) is a biologically and clinically heterogeneous blood cancer characterized by the gradual accumulation of CD5⁺ CD19⁺ malignant B cells (1, 2). Patients with an indolent form of B-CLL survive, on average, >10 years after diagnosis and often do not require immediate treatment. Patients with an aggressive form of B-CLL have an average survival of 2 years. Indolent and aggressive clinical characteristics correlate with biological characteristics including chromosomal aberrations and mutational status (the presence or absence of somatic mutations) of the immunoglobulin

variable heavy chain domain (IgV_H) of the B-cell receptor. B-CLL cells from patients with indolent clinical course typically express mutated IgV_H, whereas B-CLL cells from patients with aggressive clinical course typically express unmutated IgV_H (3, 4). In addition, expression of ZAP-70, an intracellular tyrosine kinase normally involved in T-cell activation, was shown to be a prognostic marker of the clinical course of B-CLL (5). Unmutated IgV_H and expression of ZAP-70 mRNA strongly correlated with aggressive B-CLL. Despite this clinical and biological heterogeneity, B-CLL is considered to be one disease (2).

Currently, the standard first-line treatment of B-CLL is the administration of fludarabine. Various combinations of fludarabine with cyclophosphamide and the anti-CD20 monoclonal antibody (mAb) rituximab have further increased the overall response rate and are considered steps toward managing but not curing B-CLL (6). In 2001, alemtuzumab, an anti-CD52 mAb, was approved by the Food and Drug Administration for second-line treatment of B-CLL (7–9). A number of clinical trials test various combinations of chemotherapy and mAb therapy as well as mAb therapy alone for both first-line and second-line treatment of B-CLL. Although these clinical trials are dominated by rituximab and alemtuzumab, several new mAb targeting different B-cell surface antigens, such as CD23, CD25, and CD40, have entered clinical trials.⁴ However, none of these antigens, including CD20 and CD52, are exclusively

Authors' Affiliations: ¹Experimental Transplantation and Immunology Branch and ²Metabolism Branch, Center for Cancer Research, National Cancer Institute, and ³Hematology Branch, National Heart, Lung and Blood Institute, NIH, Bethesda, Maryland

Received 7/24/07; revised 9/27/07; accepted 10/12/07.

Grant support: Intramural Research Program of the Center for Cancer Research, National Cancer Institute, NIH and the Intramural Research Program of the National Heart, Lung and Blood Institute, NIH.

The costs of publication of this article were defrayed in part by the payment of page charges. This article must therefore be hereby marked *advertisement* in accordance with 18 U.S.C. Section 1734 solely to indicate this fact.

Conflict of interest statement: The authors declare no competing financial interest.

Requests for reprints: Christoph Rader, Experimental Transplantation and Immunology Branch, Center for Cancer Research, National Cancer Institute, NIH, 9000 Rockville Pike, Building 10 CRC, Room 3-3150, Bethesda, MD 20892-1203. Phone: 301-451-2235; Fax: 301-480-3431; E-mail: raderc@mail.nih.gov.

©2008 American Association for Cancer Research.
doi:10.1158/1078-0432.CCR-07-1823

⁴ <http://www.cancer.gov/clinicaltrials/>

expressed by B-CLL cells, resulting in reduced mAb activity and increased mAb toxicity. Thus, there is a need for the discovery of unique cell surface antigens that can mediate B-CLL-specific mAb therapy.

Gene expression profiling of B-cell malignancies on a genomic scale in two independent studies (10, 11) led to the discovery of a common B-CLL signature with genes whose transcripts (*a*) were more abundant in B-CLL mRNA samples when compared with mRNA from other B-cell malignancies and normal B cells, and (*b*) were equally abundant in IgV_H-mutated and IgV_H-unmutated B-CLL mRNA samples. A fraction of these B-CLL signature genes encoded presumed cell surface proteins that may be potential target antigens for mAb therapy of B-CLL. One such B-CLL signature gene, which was discovered independently in both studies, encodes the receptor tyrosine kinase ROR1. The only other member of the ROR family (12), ROR2, shares 58% amino acid sequence identity with ROR1 but did not emerge as B-CLL signature gene. ROR1 and ROR2 are composed of a distinguished extracellular region with one immunoglobulin domain, one frizzled domain, and one kringle domain, followed by a transmembrane region and an intracellular region that contains a tyrosine kinase domain (Fig. 1B). Human and mouse ROR1 and ROR2 share 97% and 92% amino acid sequence identity, respectively (13). Gene knockout studies in mice have shown the critical roles for ROR1 and ROR2 in brain, heart, lung, and skeletal organogenesis (14, 15). Northern blotting and *in situ* hybridization analyses revealed the spatiotemporal expression pattern of ROR1 and ROR2 mRNA in embryonic mouse and rat tissues and their postnatal down-regulation (12, 16, 17). Candidate ROR1 and ROR2 ligands include secreted proteins of the Wnt family that signal through cell surface receptors with frizzled domains (18). For example, ROR2 and Wnt5a were shown to interact functionally and physically (19, 20). Functional ROR1 ligands, however, have remained unknown. Interestingly, in a recent study that used siRNAs to systematically knock down all known and putative human kinases in the human cervical cancer cell line HeLa, ROR1 emerged as an inhibitor of apoptosis (21). This finding together with the selective expression of ROR1 mRNA in B-CLL suggests a functional role in the survival of B-CLL cells. In this study, we evaluate ROR1 as a cell surface antigen for targeted therapy of human B-CLL.

Materials and Methods

Clinical samples. Untreated B-CLL patients were enrolled in an institutional review board-approved observational study protocol at the NIH, Bethesda, MD (5). Peripheral blood mononuclear cells (PBMC) were prepared from blood samples by density gradient separation on lymphocyte separation medium (ICN Biochemicals) and cryopreserved until use ($n = 32$). Matched lymph node biopsy, peripheral blood, and bone marrow aspirate specimens from four patients were also included in the analysis. PBMC from healthy donors were prepared as described above ($n = 6$). Serum samples from B-CLL patients and healthy donors were prepared from clotted blood and stored at -80°C . The IgV_H mutational status of the B-CLL cells was determined by reverse transcription-PCR (RT-PCR) followed by DNA sequencing as described elsewhere (5). DNA sequences with $>2\%$ deviation from any germ line IgV_H DNA sequence were considered mutated.

Cell lines. EBV-transformed B lymphoblastoid cell lines from normal B cells of B-CLL patients and healthy donors were established

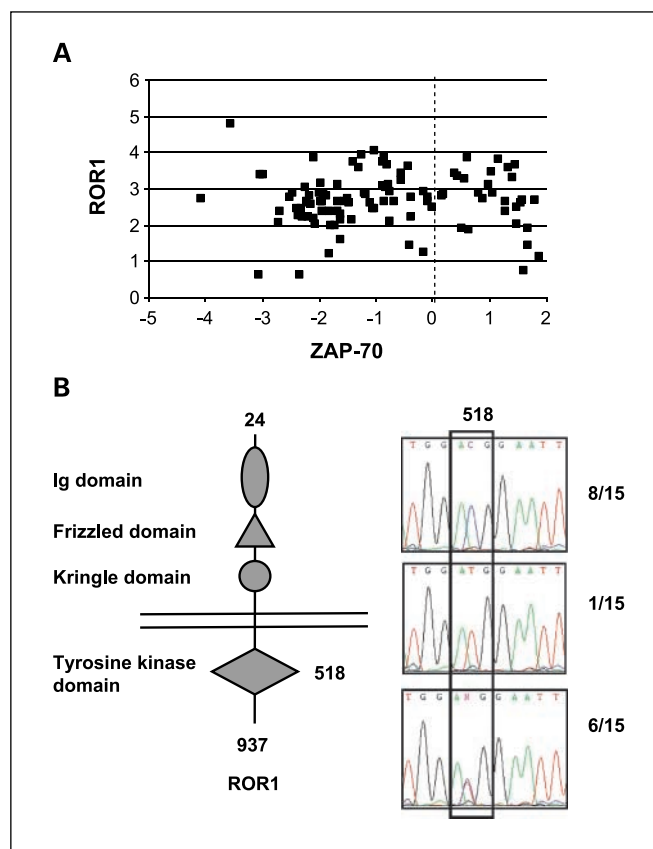


Fig. 1. ROR1 mRNA expression in B-CLL. *A*, ROR1 mRNA versus ZAP-70 mRNA expression. A cohort of 107 B-CLL patient samples (79 IgV_H mutated and 28 IgV_H unmutated) was analyzed for ROR1 versus ZAP-70 mRNA expression by gene expression profiling. ROR1 values on the y axis are given as fold expression in log₂ over the background expression level in nine pooled lymphoma cell lines (5). ZAP-70 values on the x axis are centered to the median of all samples. Dashed line, scaled cutoff between ZAP-70-negative (left) and ZAP-70-positive (right) samples as described (5). The median ROR1 mRNA expression was 6.5-fold higher (2.7 log₂) in the B-CLL patient samples compared with the nine pooled lymphoma cell lines. No significant difference in median ROR1 mRNA expression was found between ZAP-70-negative and ZAP-70-positive ($P = 0.906$) or between IgV_H-mutated and IgV_H-unmutated ($P = 0.176$) B-CLL patient samples. *B*, detection of the T518M polymorphism of ROR1 by RT-PCR followed by DNA sequencing. Left, predicted domain structure of ROR1 protein (12). Numbers, amino acid sequence of ROR1 protein before signal peptide cleavage. Right, chromatograms from three representative mRNA samples prepared from B-CLL PBMC and amplified by RT-PCR. Top, uniform ACG (threonine) allele expression found in 8 of 15 B-CLL patient samples; center, uniform ATG (methionine) allele expression found in 1 of 15 B-CLL patient samples; bottom, ACG/ATG allele expression mixture found in 6 of 15 B-CLL patient samples.

as described (22). B-CLL cell line EHEB was obtained from the German Collection of Microorganisms and Cell Cultures (23). B-CLL cell line 232-B4 was kindly provided by Dr. Anders Rosén (Linköping University, Linköping, Sweden; ref. 24). Human embryonic kidney (HEK) 293F cells (Invitrogen) were transiently transfected with a mammalian expression vector that contained the full-length cDNA of human ROR1 under control of a cytomegalovirus promoter (OriGene).

Gene expression profiling. All data from gene expression profiling presented in Fig. 1A are available online⁵ and are based on a previously published investigation on a cohort of 107 B-CLL patients (5).

RT-PCR and DNA sequencing. Total RNA was prepared from 2×10^7 PBMC using TRI Reagent (Molecular Research Center) and

⁵ <http://lmpp.nih.gov/ccl>

retrotranscribed using SuperScript III Reverse Transcriptase (Invitrogen). *ROR1* cDNA encoding fragments were amplified with FastStart Taq DNA Polymerase (Roche Applied Science) using the following seven combinations of primers: *ROR1*-1F/*ROR1*-1B, *ROR1*-1F/*ROR1*-2B, *ROR1*-2F/*ROR1*-2B, *ROR1*-2F/*ROR1*-3B, *ROR1*-3F/*ROR1*-3B, *ROR1*-3F/*ROR1*-4B, and *ROR1*-4F/*ROR1*-4B. The resulting seven overlapping *ROR1* cDNA fragments were directly analyzed by DNA sequencing using the corresponding flanking primers. For analysis of the single nucleotide polymorphism located at position 1928, primer combinations *ROR1*-2F/*ROR1*-3B and *ROR1*-3F/*ROR1*-3B were used. Listed below are the primer sequences and positions referring to *ROR1* mRNA Genbank locus NM_005012 with 5' untranslated region (1-375), coding sequence (376-3189), and 3' untranslated region (3190-3358).

ROR1-1F GCCGCCTCAGCGAGAGGAGGA (355-375)
ROR1-1B GACGGATGAAGTTTCATCGCAGTAC (1098-1074)
ROR1-2F GTACTGCGATGAAACTTCATCCGTC (1074-1098)
ROR1-2B GTCCATGCCTGGGAGATAGAGATG (1869-1846)
ROR1-3F CATCTCTATCTCCAGGCATGGAC (1846-1869)
ROR1-3B TGGGCAGTCTTCAGAGCATGTAAGAG (2529-2503)
ROR1-4F CTCTTACCATGCTCTGAAGACTGCCCA (2503-2529)
ROR1-4B CCGTCTAGTTTGTCTGTATACCAT (3234-3208)

Qualitative flow cytometry. Multiparameter flow cytometry was done in a FACSCalibur instrument (BD Biosciences; Immunocytometry Systems) using the following fluorochrome-conjugated antibodies: G1-FITC/G2a-PE, CD3-FITC/CD19-PE, and CD5-FITC/CD19-PE (two-color reagents; all from BD Biosciences); CD5-APC, CD19-FITC, CD19-PE, CD19-APC, CD80-PE, CD83-PE, CD86-PE, CD54-PE, and CD58-PE (all from BD Biosciences); and CD61-Cy5.5 (Invitrogen). Affinity-purified polyclonal goat anti-human ROR1 (g α hROR1 pAb), polyclonal goat anti-human ROR2 antibodies (g α hROR2 pAb), and polyclonal goat anti-human CD5 antibodies (g α hCD5 pAb) were used as primary antibodies (R&D Systems). Swine anti-goat-FITC (Invitrogen), donkey anti-goat-PE, and mouse anti-goat-Cy5 conjugates (Jackson ImmunoResearch Laboratories) were used as secondary antibodies. Approximately 5×10^5 cells were used for staining with appropriate primary and secondary antibodies following standard procedures, and propidium iodide was added to exclude dead cells from analysis. A total of 20,000 gated events were collected for each sample in a list mode file, and data analysis was done using CellQuest software (BD Biosciences). The values were depicted as mean fluorescence intensity (MFI).

Quantitative flow cytometry. The Quantum Simply Cellular Microbeads kit (Bangs Laboratories) was used to quantify the surface expression of ROR1 on B-CLL cells. B-CLL cells (5×10^5) were incubated with 10 μ g/mL (predetermined) g α hROR1 pAb or g α hCD5 pAb. After two washes, the cells were incubated with a 1:50 dilution (predetermined) of affinity-purified Fc-specific mouse anti-goat IgG conjugated to Cy5 (Jackson ImmunoResearch Laboratories). In addition, the cells were labeled with CD5-FITC/CD19-PE (samples stained for ROR1) or CD19-PE (samples stained for CD5) to enable gating of B-CLL cells. The peak channel fluorescence values were used to estimate the number of ROR1 or CD5 molecules on the B-CLL cell surface through their antibody binding capacity (ABC) as described below. The four bead populations in the Quantum Simply Cellular Microbeads kit were separately incubated with a predetermined saturating amount of the same secondary antibody mentioned above. The four bead populations, by virtue of having a defined number of goat anti-mouse IgG molecules on their surfaces, allowed determination of the number of secondary antibody molecules bound. Blank beads were included as instrument control. The cells and the beads were labeled at the same time and run on the same flow cytometer with the same instrument settings. A calibration curve was constructed by plotting MFI versus ABC of the beads. Using QuickCal software (Bangs Laboratories), this calibration curve then allowed the calculation of the ABC of ROR1 and CD5 on B-CLL cells.

Internalization. B-CLL cells (2×10^6) were incubated with g α hROR1 pAb for 1 h on ice. After washing thrice with ice-cold PBS containing 2% (v/v) fetal bovine serum (flow cytometry buffer) to remove unbound antibody, the cells were resuspended in flow cytometry buffer and either left on ice or incubated at 37°C for various periods of time to facilitate internalization of bound antibody. In addition, the cells were incubated at 37°C in the presence of 3 μ mol/L (predetermined) phenylarsine oxide (Sigma-Aldrich; ref. 25) or 0.09% (w/v) sodium azide to inhibit internalization of cell surface proteins. Subsequently, the cells were washed and incubated with donkey anti-goat-PE conjugate for 1 h on ice. After final three washes with flow cytometry buffer, the density of ROR1 on the cell surface was determined by MFI.

B-cell activation. Activation of B cells from B-CLL patients and healthy donors was carried out *in vitro* by incubating 5×10^6 cells with 1 μ g/mL recombinant human CD40 Ligand/TNFSF5, amino acids 108 to 261 (R&D Systems), and 500 units/mL recombinant human interleukin 4 (R&D Systems) for various periods of time (26). Control cultures were set up in parallel without the activation agents. The cells were harvested at different time points, stained for surface molecules of interest (CD80, CD83, CD86, CD54, CD58, ROR1, and ROR2), and analyzed by flow cytometry.

Cell surface biotinylation and Western blotting. Cell surface proteins from B-CLL PBMC (consisting of >95% B cells) were isolated using the Pinpoint Cell Surface Protein Isolation kit (Pierce) following the manufacturer's protocol. Purified B cells from a healthy donor, which were positively selected using CD19 beads (Miltenyi Biotech), were used as negative control. Approximately 3×10^7 cells were washed in ice-cold PBS. The cell pellet was resuspended in 30 mL of freshly prepared Sulfo-NHS-SS-Biotin solution and incubated at 4°C for 30 min with intermittent mixing. The reaction was terminated by the addition of 1.5 mL of Quenching Solution, and the cells were washed twice with TBS [25 mmol/L Tris-HCl (pH 7.2) and 150 mmol/L NaCl]. The cell pellet was resuspended in 1.5 mL of Lysis Buffer containing protease inhibitors, sonicated, incubated on ice for 30 min, and centrifuged at $10,000 \times g$ for 2 min at 4°C. The clarified supernatant containing the solubilized proteins was incubated with immobilized NeutrAvidin Gel for 1 h at room temperature by end-over-end mixing. Unbound proteins were removed by three washes with TBS containing protease inhibitors. Biotinylated proteins bound to the gel were eluted by incubation with SDS-PAGE Sample Buffer containing 50 mmol/L DTT for 1 h at room temperature and subsequent centrifugation at $1,000 \times g$ for 2 min. The eluted proteins were separated by electrophoresis in a NuPAGE Bis-Tris 4% to 12% gel (Invitrogen) and transferred to Hybond-ECL nitrocellulose membranes (GE Healthcare). The membranes were incubated overnight at 4°C with 20 mL of 1 \times Western Blocking Reagent (Roche Applied Science) in PBS, followed by 1 h incubation with 200 ng/mL g α hROR1 pAb in a rocker at room temperature. The membranes were washed thrice with 0.5% (v/v) Tween 20 in PBS and subsequently incubated with a 1:10,000 dilution of donkey anti-goat-horseradish peroxidase (HRP) conjugate (Jackson ImmunoResearch Laboratories) for 1 h at room temperature. After three washes, the membranes were developed using SuperSignal West Pico Chemiluminescent Substrate, exposed to CL-Xposure Film (Pierce), and processed in an automated developer.

Western blotting of lysates. Total cell lysate from B-CLL cells was prepared in lysis buffer [10 mmol/L Tris-HCl (pH 8.0), 130 mmol/L NaCl, 1% (v/v) Triton X-100, 5 mmol/L EDTA, and protease inhibitor cocktail (Pierce)]. After five washes, the cell pellets were resuspended in lysis buffer at 10^7 cells/mL and incubated on ice for 1 h. The lysate was cleared by centrifugation at $20,000 \times g$ and 4°C for 30 min, and the protein concentration was determined with the BCA Protein Assay kit (Pierce). B-CLL cell lysates (5 μ g total protein per lane) and normal human tissue lysates (20 μ g total protein per lane) purchased from ProSci were run on a NuPAGE Bis-Tris 4% to 12% gel under reducing condition. Western blotting was carried out with g α hROR1 pAb and donkey anti-goat-HRP conjugate as described above, except that TBS

containing 0.1% (v/v) Tween 20 was used instead of PBS in all steps. To confirm the overall protein loading of each tissue sample, duplicate membranes were probed with 200 ng/mL rabbit anti-human glyceraldehyde 3-phosphate dehydrogenase pAb (Imgenex) followed by donkey anti-rabbit-HRP conjugate (Jackson ImmunoResearch Laboratories) as described above.

Detection of soluble ROR1. A sandwich ELISA was used to detect the presence of soluble ROR1 protein in human sera. A 96-well half area plate (Costar 3690) was coated with 25 μ L/well of 2 μ g/mL rat anti-human ROR1 mAb (R&D Systems) overnight at 4°C. After several washes with distilled water, the wells were blocked with 200 μ L 3% (w/v) bovine serum albumin in PBS for 2 h at 37°C. To generate a standard curve, a recombinant fusion protein consisting of the extracellular region of human ROR1 (amino acids 24-403) fused to the COOH terminus of the Fc fragment of human IgG1 (Fc-ROR1) was cloned into mammalian expression vector pCEP4 (Invitrogen), expressed in transiently transfected HEK 293F cells, and purified by Protein A affinity chromatography as described (27). Two-fold serial dilutions of Fc-ROR1 were made in duplicate from 500 to 7.8 ng/mL. Sera from healthy donors and B-CLL patients were added to duplicate wells (25 μ L/well), and the plate was incubated for 2 h at 37°C. After several washes with wash buffer [0.05% (v/v) Tween 20 and 1% (w/v) bovine serum albumin in PBS], the wells were incubated with 25 μ L/well of 2 μ g/mL g α hROR1 pAb for 2 h at 37°C. The plate was washed several times with wash buffer and distilled water, and incubated with 25 μ L/well of a 1:2,000 dilution of donkey anti-goat-HRP conjugate for 1 h at 37°C. After 10 to 15 washes, 25 μ L/well of freshly prepared substrate solution [2,2'-azino-bis(3-ethylbenzthiazoline)-6-sulfonic acid; Roche Applied Science] was added, incubated for 10 min, and the absorbance was measured at 405 nm with a wavelength correction set at 490 nm using a VersaMax microplate reader (Molecular Devices). The data were analyzed using SoftMax Pro software (Molecular Devices).

Results

ROR1 mRNA expression in B-CLL. We first used gene expression profiling to confirm and extend the previously published ROR1 mRNA expression in B-CLL (10, 11). A cohort of 107 B-CLL patient samples was analyzed for ROR1 versus ZAP-70 mRNA expression using Lymphochip DNA microarrays as described (5). ROR1 mRNA was highly expressed in all B-CLL samples regardless of ZAP-70 mRNA expression and IgV_H mutational status (Fig. 1A). ROR2 mRNA expression was not detected in any of the samples tested (data not shown). To confirm the integrity of B-CLL-derived ROR1 mRNA, we amplified the entire 2.8-kb coding sequence by RT-PCR as a series of overlapping ROR1 cDNA encoding fragments and verified them by DNA sequencing ($n = 2$). Confirming the restricted ROR1 mRNA expression in B-CLL (Fig. 1A; refs. 10, 11), mRNA derived from healthy donor PBMC did not yield any RT-PCR products, indicating the absence of full-length or differentially spliced ROR1 mRNAs (data not shown).

We next analyzed the B-CLL ROR1 mRNA for the only validated single nucleotide polymorphism that results in an amino acid sequence polymorphism (rs7527017).⁶ The single nucleotide polymorphism is a C or T at mRNA position 1928, resulting in an ACG (threonine) or ATG (methionine) codon at amino acid position 518 within the intracellular tyrosine kinase domain of ROR1 (T518M polymorphism). In the normal population ($n = 317$), across ethnicities, an allele frequency of

73.6% ACG and 26.4% ATG, and a genotype frequency of 57.4% ACG/ACG, 35.0% ACG/ATG, and 7.6% ATG/ATG was found. We analyzed B-CLL ROR1 mRNA from 15 patients by RT-PCR amplification and subsequent DNA sequencing of a ROR1 cDNA fragment that encompassed the single nucleotide polymorphism of interest. As shown in Fig. 1B, DNA sequencing allowed us to detect the presence of either a uniform allele sequence (homozygous ACG or ATG) or an even mixture of two allele sequences (heterozygous ACG/ATG). Out of 15 B-CLL patients, 9 revealed a homozygous allele expression with ACG found in 8 patients (53%) and ATG found in 1 patient (7%). The remaining six patients (40%) were heterozygous, expressing an ACG/ATG allele mixture. This distribution accurately matched the genotype frequency reported in the normal population (see above). Moreover, there was no correlation of ROR1 T518M polymorphism and IgV_H mutational status (data not shown), suggesting that the ROR1 T518M polymorphism does not associate with prognostically distinct B-CLL subtypes.

Restricted and uniform expression of ROR1 protein on the surface of B-CLL cells. To analyze the cell surface expression of ROR1 protein by flow cytometry, we first validated the selective binding of commercially available g α hROR1 pAb to HEK 293F cells transiently transfected with a mammalian expression vector that contained the full-length cDNA of human ROR1 under control of a cytomegalovirus promoter. Normal goat immunoglobulin and g α hROR2 pAb were used as controls. Whereas untransfected HEK 293F cells revealed weak staining with both g α hROR1 pAb and g α hROR2 pAb, HEK 293F/ROR1 cells showed strongly enhanced staining for ROR1 but not ROR2 (data not shown).

We next analyzed PBMC prepared from 32 untreated B-CLL patients for ROR1 protein expression on the surface of B-CLL cells. Consistent with the gene expression profiling studies, g α hROR1 pAb detected ROR1 protein on the surface of B-CLL cells (CD5⁺ CD19⁺), but not on normal B cells (CD5⁻ CD19⁺), T cells (CD5⁺ CD19⁻), or CD5⁻ CD19⁻ PBMC from B-CLL patients (Fig. 2A). Normal goat immunoglobulin and g α hROR2 pAb served as specificity controls and did not bind to B-CLL cells as expected (Fig. 2A). In addition, PBMC and CD61⁺ platelets from healthy donors were negative for cell surface ROR1 (data not shown).

To independently confirm the cell surface expression of ROR1 and to show ROR1 protein integrity, we used a combination of cell surface biotinylation and Western blotting. Whole PBMC from a B-CLL patient were first treated with a biotinylation reagent. After cell lysis, the biotinylated cell surface proteins were isolated with NeutrAvidin and separated by SDS-PAGE. Subsequent Western blotting with g α hROR1 pAb and donkey anti-goat-HRP conjugate detected a single band with a molecular mass of ~120 kDa (Fig. 2B). The same band was found for HEK 293F/ROR1 transfectants (data not shown) and COS/ROR1 transfectants (12). Western blotting with g α hROR2 pAb followed by the same secondary antibodies did not yield a band (data not shown), confirming the absence of B-CLL cell surface ROR2. ROR1 protein was not detected in B cells enriched from healthy donor PBMC, revealing once more the restricted expression of ROR1 protein in B-CLL cells (Fig. 2B).

To investigate whether B-CLL cell surface ROR1 can mediate antibody internalization, B-CLL cells were incubated with

⁶ <http://www.ncbi.nlm.nih.gov/SNP>

g α hROR1 pAb, washed, and either left on ice or incubated at 37°C for various periods of time. Subsequent staining with donkey anti-goat-PE conjugate showed reduction of ROR1 on the cell surface only in samples incubated at 37°C after as early as 1 h (Fig. 2C). The reduction of cell surface ROR1 was completely blocked by the addition of endocytosis inhibitors phenylarsine oxide (Fig. 2C) and sodium azide (data not shown). These results indicate that cell surface ROR1 can mediate at least partial internalization of bound antibody by endocytosis.

The restricted expression of ROR1 protein on the surface of B-CLL cells was confirmed in all patients tested, including 15

with IgV_H mutated and 13 with IgV_H unmutated status (Fig. 3A). Despite biological and clinical heterogeneity as well as wide range of lymphocyte counts in these patients, the level of ROR1 cell surface expression was within a relatively narrow range, three to five times above background. As shown above for ROR1 mRNA, there was no significant difference in ROR1 protein expression between IgV_H mutated and IgV_H unmutated status (Fig. 3A). Although the level of ROR1 protein expression varied between the B-CLL patients, all B-CLL cells in a given patient expressed strikingly uniform levels as indicated by very narrow histogram profiles (Fig. 2A). This uniformity was also found among B-CLL cells obtained from different anatomic

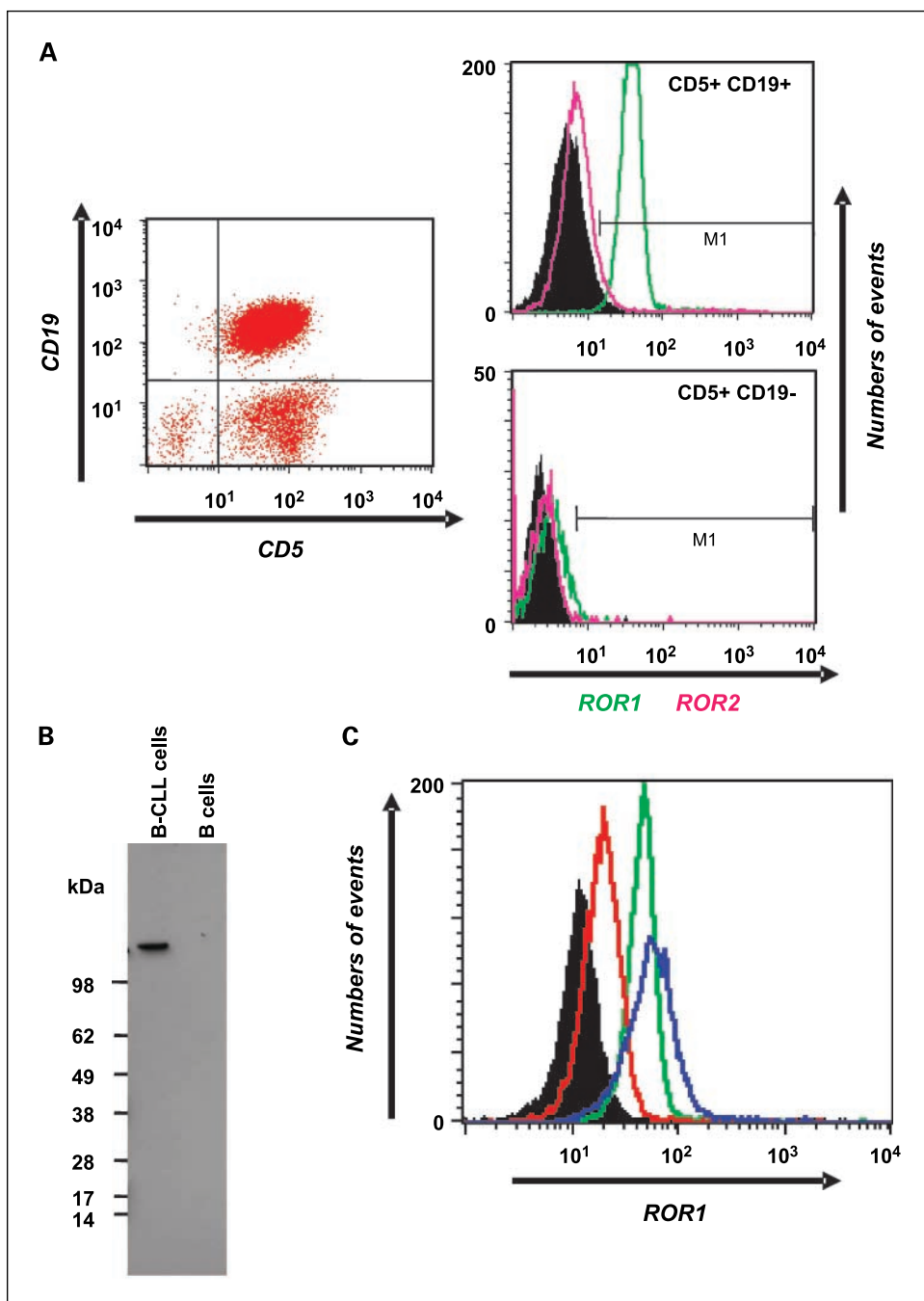


Fig. 2. ROR1 protein expression on the surface of B-CLL cells. *A*, flow cytometry profiles of PBMC from a representative B-CLL patient. Four-color flow cytometry was carried out with a mouse anti-human CD5 mAb conjugated to PE, a mouse anti-human CD19 mAb conjugated to APC, g α hROR1 pAb or g α hROR2 pAb, swine anti-goat-FITC conjugate, and propidium iodide. The histograms on the right represent staining for ROR1 (green) and ROR2 (pink) in CD5⁺ CD19⁺ B-CLL cells (top) and CD5⁺ CD19⁻ T cells (bottom). The background signal with normal goat immunoglobulin or secondary antibody alone is shown in black. *B*, biotinylated cell surface proteins from B-CLL cells or normal B cells were separated by SDS-PAGE. Subsequent Western blotting with g α hROR1 pAb and donkey anti-goat-HRP conjugate detected a single band of ~120 kDa in B-CLL cells (left lane). No band was detected in normal B cells (right lane). *C*, B-CLL cells were incubated with g α hROR1 pAb for 1 h at 4°C. Subsequently, the cells were washed and either left at 4°C (green) or incubated for 1 h at 37°C in the absence (red) or presence (blue) of 3 μ mol/L phenylarsine oxide, followed by flow cytometry analysis with swine anti-goat-FITC conjugate. The background signal with secondary antibody alone is shown in black.

Downloaded from <http://aacrjournals.org/clincancerres/article-pdf/14/2/396/1976743/396.pdf> by guest on 06 November 2024

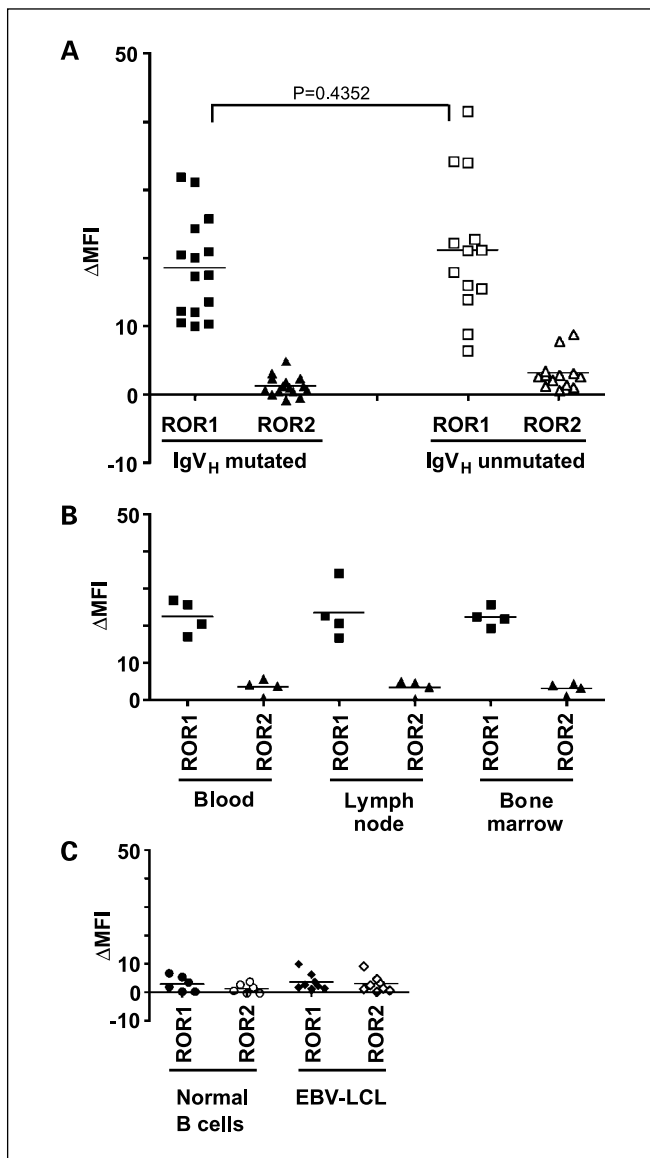


Fig. 3. ROR1 protein expression on the surface of B-CLL cells is independent of IgV_H mutational status and anatomic niches. **A**, PBMC from IgV_H-mutated ($n = 15$) and IgV_H-unmutated ($n = 13$) B-CLL patients were stained for ROR1 and ROR2 as described in Fig. 2. Δ MFI, the MFI of α hROR1 or α hROR2 pAb minus the MFI obtained with normal goat immunoglobulin. Each data point depicts the MFI of an individual B-CLL sample obtained with α hROR1 pAb or α hROR2 pAb minus the MFI obtained with normal goat immunoglobulin. **B**, paired samples of blood, lymph node, and bone marrow were obtained from 4 B-CLL patients, and the MFIs were determined as before. **C**, normal B cells from six healthy donors (*left*) and two EBV-transformed B lymphoblastoid cell lines established from healthy donors as well as 6 EBV-transformed B lymphoblastoid cell lines established from B-CLL patients (*EBV-LCL; right*) were analyzed as before. The latter included the two previously reported EBV-transformed B-CLL cell lines EHEB and 232-B4 (23, 24). Horizontal lines, arithmetic mean values.

niches, i.e., peripheral blood, lymph node, and bone marrow (Fig. 3B).

Next, we were interested in determining whether ROR1 protein expression was associated with the transformation process of human B cells. Purified B cells from healthy donors were negative for cell surface ROR1 (Fig. 3C). EBV-transformed B lymphoblastoid cell lines established *in vitro* from normal B cells of healthy donors and B-CLL patients were negative for

both ROR1 protein (Fig. 3C) and *ROR1* mRNA (data not shown) expression. Thus, EBV transformation did not induce ROR1 protein or *ROR1* mRNA expression. In addition, two previously described EBV-transformed B-CLL cell lines, which were reported to express the same monoclonal IgV_H as the malignant B cells (23, 24), did not express ROR1 protein (Fig. 3C) or *ROR1* mRNA (data not shown).

To quantify the expression of B-CLL cell surface ROR1 in terms of ABC, we used polyclonal antibodies and calibration beads (see Materials and Methods). Samples from B-CLL patients with high and low cell surface ROR1 levels (Fig. 3A) were included in this analysis, and staining for cell surface CD5 was used as a reference. Based on a standard curve obtained with the calibration beads, the ABC of B-CLL cell surface ROR1 was calculated to be in the range of 10^3 to 10^4 molecules per cell (2,773-7,090 molecules per cell; Table 1). Using corresponding polyclonal antibodies, the ABC of B-CLL cell surface CD5 was calculated to be three to five times higher (7,362-21,002 molecules per cell). Validating our quantitative analysis, the ABC of B-CLL cell surface CD5 was found to be in close agreement with a recent study that was based on mAb and a larger cohort of B-CLL patients (28).

Constitutive expression of ROR1 protein on the surface of B-CLL cells. Although ROR1 protein was not detected in normal B cells and EBV-transformed B lymphoblastoid cell lines, it remained possible that B-cell activation may induce ROR1 protein expression in normal B cells. In addition, activation of B-CLL cells might up- or down-regulate ROR1 protein expression on their cell surface. We first analyzed the expression of cell surface ROR1 on normal B cells and B-CLL cells in the absence of any B-cell activation >5 days in culture. ROR1 protein expression by B-CLL cells was remarkably stable during this period, whereas normal B cells remained negative (Fig. 4). Activation of B cells with soluble CD40L plus interleukin 4 induced up-regulation of a number of costimulatory molecules such as CD80, CD83, CD86, CD54, and CD58 in both B-CLL cells and normal B cells (Fig. 4 and data not shown). However, this activation failed to induce ROR1 protein expression in normal B cells or alter ROR1 protein expression in B-CLL cells (Fig. 4). Furthermore, despite variation in the levels of CD80 expression after activation of B-CLL cells from different patients, there was no significant change in ROR1 protein expression (data not shown).

ROR1 protein expression in normal adult tissues. For the development of targeted therapeutics, it was important to know whether ROR1 protein is expressed on the surface of normal

Table 1. ABC of B-CLL cell surface ROR1

B-CLL sample	ABC for CD5	ABC for ROR1
1	Not determined	7,090*
2	8,872	4,551
3	14,720	2,773
4	16,002	3,993
5	7,362	3,315
6	21,002	4,164

*ABC values indicate molecules per cell and are representative of at least two independent measurements.

cells. Although our flow cytometry and cell surface biotinylation experiments showed that normal blood cells do not express cell surface ROR1 (Figs. 2B, 3C, and 4; data not shown), we sought to extend the study to other normal adult tissues. Lysates of PBMC from B-CLL patients were compared with lysates of 28 normal adult tissues by Western blotting (Fig. 5). A ~120-kDa band that specifies cell surface ROR1 as revealed by cell surface biotinylation (Fig. 2B) was prominent in B-CLL PBMC. This band was absent in the majority of normal adult tissues even with four times higher protein loading (Fig. 5). However, it remains possible that cell surface ROR1 is expressed at very low levels in testis, uterus, lung, bladder, and colon as indicated by faint bands in the range of 100 to 150 kDa (Fig. 5). A higher molecular weight band was detected in adipose tissue, whereas lower molecular weight bands, including a prominent ~50-kDa band, were detected in B-CLL PBMC and most of the normal adult tissues (Fig. 5). It is possible that the ~50-kDa band originates from a splice variant of ROR1 that was recently discovered *in silico* (Genbank locus NM_001083592). This splice variant does not encode a cell surface protein. Fittingly, the ~50-kDa band was not detected by cell surface biotinylation (Fig. 2B).

Detection of soluble ROR1 protein. The presence of soluble ROR1 protein in circulation could compromise the efficacy of targeted therapeutics. To address this possibility, we developed a sandwich ELISA to detect the presence of soluble ROR1 protein in the serum of B-CLL patients as well as healthy donors. For this, soluble ROR1 protein was first captured with a

rat anti-human ROR1 mAb and then detected with goat anti-rat ROR1 pAb followed by donkey anti-goat-HRP conjugate. Using a recombinant human Fc-ROR1 fusion protein for standardization, this sandwich ELISA enabled us to detect and quantify soluble ROR1 in human sera at concentrations as low as 10 ng/mL with a linear range from 25 to 250 ng/mL. Fourteen of eighteen (>75%) serum samples from untreated B-CLL patients did not contain detectable levels of soluble ROR1 protein. The remaining four sera showed low levels of soluble ROR1 in a concentration range of 37 to 191 ng/mL. No correlation was found between the concentration of soluble ROR1 protein and lymphocyte counts or IgV_H mutational status (data not shown). Moreover, we also detected similar low levels (23-169 ng/mL) of soluble ROR1 protein in 3 of 17 healthy donor sera. The source of these low levels of soluble ROR1 protein in <25% of B-CLL patients and in a similar fraction of healthy donors is uncertain.

Discussion

Restricted, uniform, and constitutive cell surface expression are key features of antigens targeted by mAb therapy (7, 29). Thus, our study provides an incentive to develop human, humanized, or chimeric mAb to ROR1 for B-CLL therapy. Other mAb currently used for B-CLL therapy are rituximab, which targets CD20, and alemtuzumab, which targets CD52 (8). Although these mAb have fewer side effects than standard chemotherapy, which is an important consideration for the

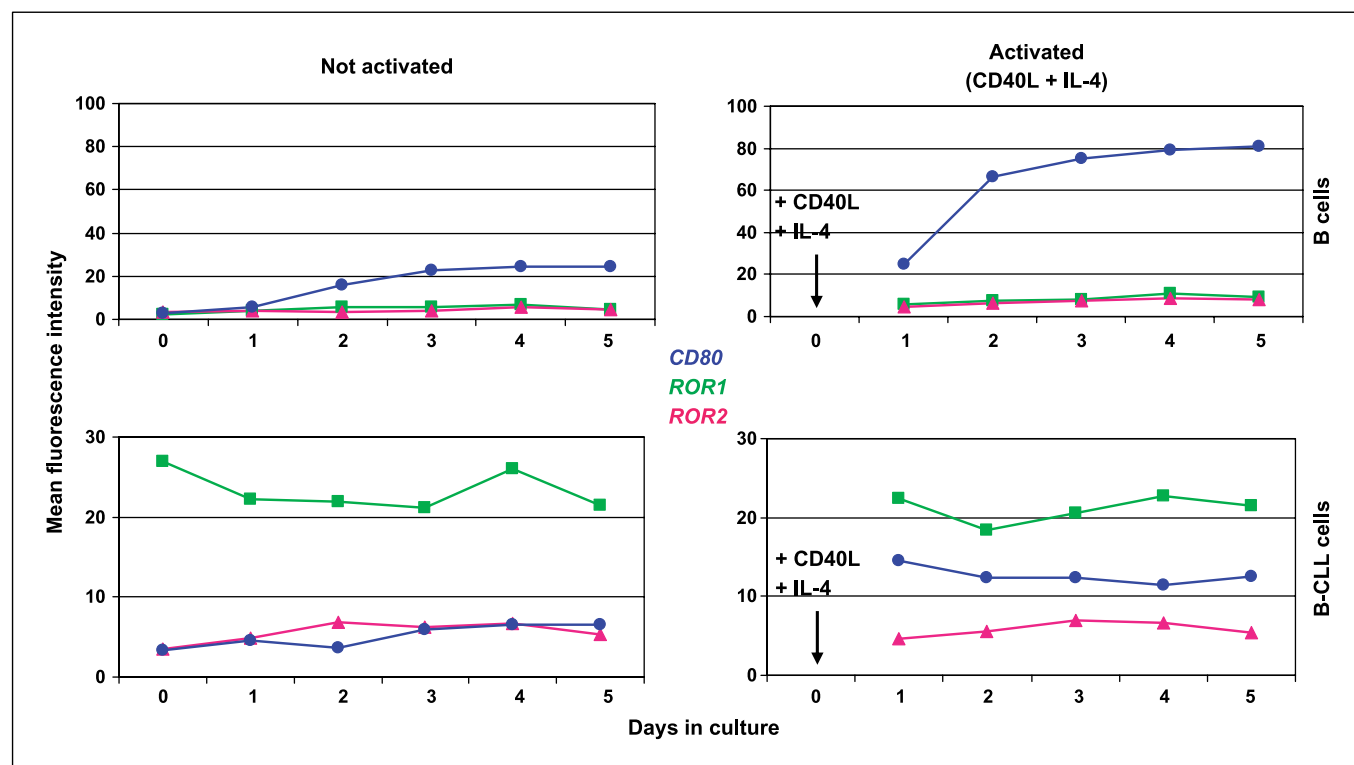
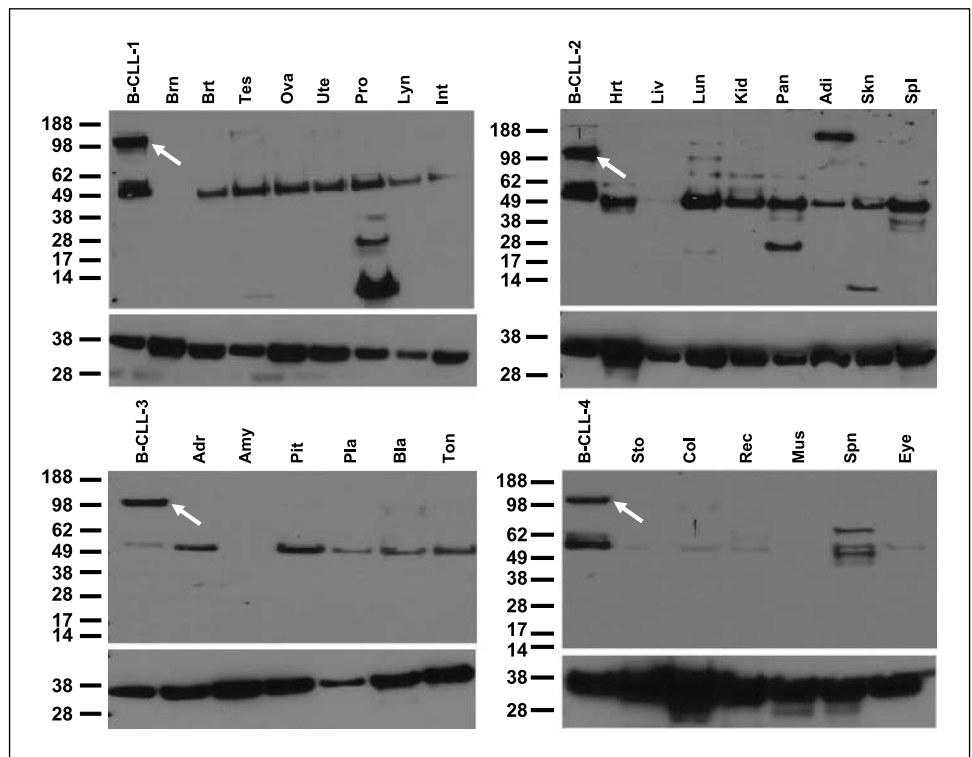


Fig. 4. ROR1 protein expression on the surface of B-CLL cells is not modulated by B-cell activation. B cells or B-CLL cells (5×10^6 per well) were cultured in the absence or presence of 1 μ g/mL soluble recombinant human CD40L protein and 500 units/mL recombinant human interleukin 4. Cells were harvested at indicated time points, stained, and analyzed by flow cytometry. Expression of surface CD80 (blue circles), ROR1 (green squares), and ROR2 (pink triangles) on normal B cells (top) and B-CLL cells (bottom) without (left) or with B-cell activation (right). CD19⁺ B cells, regardless of their expression levels of CD80, were gated for analysis. The data are representative of three healthy donors and five B-CLL patients studied.

Fig. 5. Normal adult tissues do not express cell surface ROR1. Lysates from PBMC of B-CLL patients (5 μ g total protein per lane) were compared with lysates from 28 normal adult tissues (20 μ g total protein per lane) by Western blotting using goatROR1 pAb followed by donkey anti-goat-HRP conjugate. Arrows, ~120-kDa band that specifies cell surface ROR1 (Fig. 2B). Rabbit anti-human glyceraldehyde-3-phosphate dehydrogenase pAb followed by donkey anti-rabbit-HRP conjugate were used as positive control (*bottom*). Normal adult tissues: Brn, brain; Brt, breast; Tes, testis; Ova, ovary; Ute, uterus; Pro, prostate; Lyn, lymph node; Int, small intestine; Hrt, heart; Liv, liver; Lun, lung; Kid, kidney; Pan, pancreas; Adi, adipose; Skn, skin; Spl, spleen; Adr, adrenal gland; Amy, amygdala; Pit, pituitary gland; Pla, placenta; Bla, bladder; Ton, tonsil; Sto, stomach; Col, colon; Rec, rectum; Mus, skeletal muscle; Spn, spinal cord; Eye, eye.



largely older B-CLL patient population, they also target normal CD20⁺ B cells and CD52⁺ B cells, T cells, natural killer cells, and monocytes, respectively. Due to the ubiquitous expression of CD52 on lymphocytes and monocytes, alemtuzumab significantly suppresses the immune system, often leading to reactivation of latent viruses and opportunistic infections (7). By contrast, therapeutic mAb to ROR1 could facilitate B-CLL-specific targeting with fewer side effects. We determined that the ABC of B-CLL cell surface ROR1 among different patients is in the range of 10^3 to 10^4 molecules per cell. Notably, ROR1 protein expression on B-CLL cells within any given patient was strikingly homogenous and also uniform among B-CLL cells from different anatomic niches. By comparison, the ABC of B-CLL cell surface CD5 and CD20, albeit more heterogeneous, were found to be in the 1 to 2×10^4 molecules per cell range (28, 30). The relatively lower cell surface density of ROR1 protein may limit antibody-mediated immune effector functions, including complement-dependent cytotoxicity and antibody-dependent cellular cytotoxicity. However, the restricted expression of ROR1 protein on B-CLL cells clearly distinguishes ROR1 from CD20 and CD52, and may allow specific mAb targeting and enhanced effector functions through conjugated radioisotopes (31), chemotherapeutic agents (32), or bacterial toxins (33). In fact, our finding that cell surface ROR1 can mediate antibody internalization makes the selective delivery of such cytotoxic agents through ROR1 targeting particularly appealing.

A concern for mAb therapy is the presence of soluble antigen that is shed or secreted from cells and potentially reduces the number of mAb molecules available for cell surface targeting. We did not detect soluble ROR1 protein in >75% of sera from B-CLL patients. Even the low concentrations (<200 ng/mL) of

soluble ROR1 protein we found in <25% of sera from B-CLL patients are unlikely to interfere with mAb therapy, considering that mAb therapy usually operates with mAb serum concentrations in the μ g/mL range. For example, in clinical trials leading to the approval of alemtuzumab for B-CLL therapy, the mAb was given i.v. at a dose of thrice 30 mg per week for 12 weeks (34, 35). In contrast to soluble ROR1, soluble CD52 was detected in sera from B-CLL patients at concentrations (1-200 μ g/mL) high enough to interfere with the binding of alemtuzumab to B-CLL cells *in vitro* (36). Furthermore, unlike soluble ROR1, soluble CD52 and also soluble CD23 are considerably elevated in sera from B-CLL patients when compared with healthy donor sera and correlate with biological and clinical characteristics (36).

The restricted, uniform, and constitutive cell surface expression of ROR1 in B-CLL, together with a systematic siRNA screen from which ROR1 emerged as inhibitor of apoptosis in the human cervical cancer cell line HeLa (21), suggest a functional role for ROR1 protein in the survival of B-CLL cells. Future studies will address whether mAb that target ROR1 protein can directly interfere with B-CLL cell survival. Two mAb approved by the Food and Drug Administration that not only bind but antagonize receptor tyrosine kinases are trastuzumab, which binds to ERBB2, and cetuximab, which binds to epidermal growth factor receptor (37, 38). Taken together, our findings warrant ROR1 to be an attractive target for B-CLL therapy.

Acknowledgments

We thank Therese White for outstanding support in procuring patient samples, the Department of Transfusion Medicine for providing blood samples from healthy donors, Dr. William G. Telford and Veena Kapoor for maintaining the flow cytometry core facility, and Dr. Anders Rosén for providing the 232-B4 cell line.

References

1. Winkler D, Dohner H, Stilgenbauer S. Genetics, gene expression, and targeted therapies in chronic lymphocytic leukemia. *Curr Drug Targets* 2006;7:1313–27.
2. Binet JL, Caligaris-Cappio F, Catovsky D, et al. Perspectives on the use of new diagnostic tools in the treatment of chronic lymphocytic leukemia. *Blood* 2006;107:859–61.
3. Damle RN, Wasil T, Fais F, et al. Ig V gene mutation status and CD38 expression as novel prognostic indicators in chronic lymphocytic leukemia. *Blood* 1999;94:1840–7.
4. Hamblin TJ, Davis Z, Gardiner A, Oscier DG, Stevenson FK. Unmutated Ig V(H) genes are associated with a more aggressive form of chronic lymphocytic leukemia. *Blood* 1999;94:1848–54.
5. Wiestner A, Rosenwald A, Barry TS, et al. ZAP-70 expression identifies a chronic lymphocytic leukemia subtype with unmutated immunoglobulin genes, inferior clinical outcome, and distinct gene expression profile. *Blood* 2003;101:4944–51.
6. Elter T, Hallek M, Engert A. Fludarabine in chronic lymphocytic leukaemia. *Expert Opin Pharmacother* 2006;7:1641–51.
7. O'Mahony D, Bishop MR. Monoclonal antibody therapy. *Front Biosci* 2006;11:1620–35.
8. Cheson BD. Monoclonal antibody therapy of chronic lymphocytic leukemia. *Cancer Immunol Immunother* 2006;55:188–96.
9. Lundin J, Osterborg A. Advances in the use of monoclonal antibodies in the therapy of chronic lymphocytic leukemia. *Semin Hematol* 2004;41:234–45.
10. Klein U, Tu Y, Stolovitzky GA, et al. Gene expression profiling of B cell chronic lymphocytic leukemia reveals a homogeneous phenotype related to memory B cells. *J Exp Med* 2001;194:1625–38.
11. Rosenwald A, Alizadeh AA, Widhopf G, et al. Relation of gene expression phenotype to immunoglobulin mutation genotype in B cell chronic lymphocytic leukemia. *J Exp Med* 2001;194:1639–47.
12. Masiakowski P, Carroll RD. A novel family of cell surface receptors with tyrosine kinase-like domain. *J Biol Chem* 1992;267:26181–90.
13. Forrester WC. The Ror receptor tyrosine kinase family. *Cell Mol Life Sci* 2002;59:83–96.
14. Nomi M, Oishi I, Kani S, et al. Loss of mRor1 enhances the heart and skeletal abnormalities in mRor2-deficient mice: redundant and pleiotropic functions of mRor1 and mRor2 receptor tyrosine kinases. *Mol Cell Biol* 2001;21:8329–35.
15. Takeuchi S, Takeda K, Oishi I, et al. Mouse Ror2 receptor tyrosine kinase is required for the heart development and limb formation. *Genes Cells* 2000;5:71–8.
16. Al-Shawi R, Ashton SV, Underwood C, Simons JP. Expression of the Ror1 and Ror2 receptor tyrosine kinase genes during mouse development. *Dev Genes Evol* 2001;211:161–71.
17. Matsuda T, Nomi M, Ikeya M, et al. Expression of the receptor tyrosine kinase genes, Ror1 and Ror2, during mouse development. *Mech Dev* 2001;105:153–6.
18. Wang HY, Liu T, Malbon CC. Structure-function analysis of Frizzleds. *Cell Signal* 2006;18:934–41.
19. Oishi I, Suzuki H, Onishi N, et al. The receptor tyrosine kinase Ror2 is involved in non-canonical Wnt5a/JNK signalling pathway. *Genes Cells* 2003;8:645–54.
20. Nishita M, Yoo SK, Nomachi A, et al. Filopodia formation mediated by receptor tyrosine kinase Ror2 is required for Wnt5a-induced cell migration. *J Cell Biol* 2006;175:555–62.
21. MacKeigan JP, Murphy LO, Blenis J. Sensitized RNAi screen of human kinases and phosphatases identifies new regulators of apoptosis and chemoresistance. *Nat Cell Biol* 2005;7:591–600.
22. Aman P, Ehlin-Henriksson B, Klein G. Epstein-Barr virus susceptibility of normal human B lymphocyte populations. *J Exp Med* 1984;159:208–20.
23. Saltman D, Bansal NS, Ross FM, Ross JA, Turner G, Guy K. Establishment of a karyotypically normal B-chronic lymphocytic leukemia cell line; evidence of leukemic origin by immunoglobulin gene rearrangement. *Leuk Res* 1990;14:381–7.
24. Wendel-Hansen V, Sallstrom J, De Campos-Lima PO, et al. Epstein-Barr virus (EBV) can immortalize B-cll cells activated by cytokines. *Leukemia* 1994;8:476–84.
25. Gibson AE, Noel RJ, Herlihy JT, Ward WF. Phenylarsine oxide inhibition of endocytosis: effects on asialofetuin internalization. *Am J Physiol* 1989;257:C182–4.
26. Buhmann R, Nolte A, Westhaus D, Emmerich B, Hallek M. CD40-activated B-cell chronic lymphocytic leukemia cells for tumor immunotherapy: stimulation of allogeneic versus autologous T cells generates different types of effector cells. *Blood* 1999;93:1992–2002.
27. Hofer T, Tangkeangsirisin W, Kennedy MG, et al. Chimeric rabbit/human Fab and IgG specific for members of the Nogo-66 receptor family selected for species cross-reactivity with an improved phage display vector. *J Immunol Methods* 2007;318:75–87.
28. Olejniczak SH, Stewart CC, Donohue K, Czuczman MS. A quantitative exploration of surface antigen expression in common B-cell malignancies using flow cytometry. *Immunol Invest* 2006;35:93–114.
29. Carter PJ. Potent antibody therapeutics by design. *Nat Rev Immunol* 2006;6:343–57.
30. Wang L, Abbasi F, Gaigalas AK, Vogt RF, Marti GE. Comparison of fluorescein and phycoerythrin conjugates for quantifying CD20 expression on normal and leukemic B-cells. *Cytometry B Clin Cytom* 2006;70:410–5.
31. Milenic DE, Brady ED, Brechbiel MW. Antibody-targeted radiation cancer therapy. *Nat Rev Drug Discov* 2004;3:488–99.
32. Wu AM, Senter PD. Arming antibodies: prospects and challenges for immunoconjugates. *Nat Biotechnol* 2005;23:1137–46.
33. Pastan I, Hassan R, Fitzgerald DJ, Kreitman RJ. Immunotoxin therapy of cancer. *Nat Rev Cancer* 2006;6:559–65.
34. Osterborg A, Dyer MJ, Bunjes D, et al. European Study Group of CAMPATH-1H Treatment in Chronic Lymphocytic Leukemia. Phase II multicenter study of human CD52 antibody in previously treated chronic lymphocytic leukemia. *J Clin Oncol* 1997;15:1567–74.
35. Rai KR, Freter CE, Mercier RJ, et al. Alemtuzumab in previously treated chronic lymphocytic leukemia patients who also had received fludarabine. *J Clin Oncol* 2002;20:3891–7.
36. Albitar M, Do KA, Johnson MM, et al. Free circulating soluble CD52 as a tumor marker in chronic lymphocytic leukemia and its implication in therapy with anti-CD52 antibodies. *Cancer* 2004;101:999–1008.
37. Cho HS, Mason K, Ramyar KX, et al. Structure of the extracellular region of HER2 alone and in complex with the Herceptin Fab. *Nature* 2003;421:756–60.
38. Li S, Schmitz KR, Jeffrey PD, Wiltzius JJ, Kussie P, Ferguson KM. Structural basis for inhibition of the epidermal growth factor receptor by cetuximab. *Cancer Cell* 2005;7:301–11.